Functional and biophysical analyses of the class XIV Toxoplasma gondii myosin D

Herm-Götz, Angelika; Delbac, Frêdêric; Weiss, Stefan; Nyitrai, Miklos; Stratmann, Rolf; Tomavo, Stanislas; Sibley, L David; Geeves, Michael A; Soldati-Favre, Dominique

How to cite

HERM-GÖTZ, Angelika et al. Functional and biophysical analyses of the class XIV Toxoplasma gondii myosin D. In: Journal of muscle research and cell motility, 2006, vol. 27, n° 2, p. 139–151. doi: 10.1007/s10974-005-9046-1

This publication URL: https://archive-ouverte.unige.ch//unige:78025
Publication DOI: 10.1007/s10974-005-9046-1

Journal of Muscle Research and Cell Motility (2006) 27:139–151
DOI 10.1007/s10974-005-9046-1

Functional and biophysical analyses of the class XIV *Toxoplasma gondii* Myosin D

ANGELIKA HERM-GÖTZ[1,2], FRÉDÉRIC DELBAC[1,3], STEFAN WEISS[4], MIKLOS NYITRAI[4,7], ROLF STRATMANN[2,8], STANISLAS TOMAVO[5], L. DAVID SIBLEY[6], MICHAEL A. GEEVES[4] and DOMINIQUE SOLDATI[2,9,*]

[1]*Hygieneinstitut, Universitätsklinikum Heidelberg, Im Neuenheimer Feld 324, D-69120, Heidelberg, Germany;* [2]*Zentrum für Molekulare Biologie, Universität Heidelberg, Im Neuenheimer Feld 282, D-69120, Heidelberg, Germany;* [3]*Laboratoire Biologie des Protistes, UMR CNRS 6023, Université Blaise Pascal, 24 av. des Landais, 63177, Aubière cedex, France;* [4]*Department of Biosciences, University of Kent, CT2 7NJ, Canterbury, UK;* [5]*Laboratoire de Chimie Biologique CNRS UMR 8576, Bâtiment C9 Université des Sciences et Technologies de Lille, 59655, Villeneuve d'Ascq, France;* [6]*Department of Molecular Microbiology, Washington University School of Medicine, St. Louis, MO, 63110, USA;* [7]*Department of Biophysics, University of Pécs, Pécs, Hungary;* [8]*Heidelberger Institut für Pflanzenwissenschaften, Universität Heidelberg, Im Neuenheimer Feld 360, D-69120, Heidelberg, Germany;* [9]*Department of Microbiology and Molecular Medicine, Faculty of Medicine, University of Geneva CMU, 1 Rue Michel-Servet, 1211, Geneva 4, Switzerland*

Received 2 September 2005; accepted in revised form 26 October 2005

Summary

The obligate intracellular parasite *Toxoplasma gondii* uses gliding motility to migrate across the biological barriers of the host and to invade cells. This unique form of locomotion requires an intact actin cytoskeleton and involves at least one motor protein (TgMyoA) that belongs to the class XIV of the myosin superfamily. TgMyoA is anchored in the inner membrane complex and is essential for the gliding motion, host cell invasion and egress of *T. gondii* tachyzoites. TgMyoD is the smallest *T. gondii* myosin and is structurally very closely related to TgMyoA. We show here that TgMyoD exhibits similar transient kinetic properties as the fast single-headed TgMyoA. To determine if TgMyoD also contributes to parasite gliding motility, the *TgMyoD* gene was disrupted by double homologous recombination. In contrast to *TgMyoA*, *TgMyoD* gene is dispensable for tachyzoite propagation and motility. Parasites lacking TgMyoD glide normally and their virulence is not compromised in mice. The fact that TgMyoD is predominantly expressed in bradyzoites explains the absence of a phenotype observed with *myodko* in tachyzoites and does not exclude a role of this motor in gliding that would be restricted to the cyst forming but nevertheless motile stage of the parasite.

Abbreviations: BDM – butanedione monoxime; mant ATP – *N-methylanthraniloyl derivatives of 2′deoxy-ATP*

Introduction

Toxoplasma gondii is an obligate intracellular protozoan parasite belonging to the phylum *Apicomplexa*. It is known as an important human, and veterinary pathogen, mainly responsible for opportunistic infections in AIDS patients and causing diseases in congenitally infected infants (Luft and Remington, 1992). Like other apicomplexans, *T. gondii* uses gliding motility as a way to penetrate biological barriers and to actively enter into host cells. Invasion is mediated by the translocation of transmembrane adhesins from the apical pole where they are discharged by the micronemes to the posterior pole of the parasite (Carruthers and Sibley, 1997). This substrate-dependent motion was previously demonstrated to require an intact parasite actin cytoskeleton (Dobrowolski and Sibley, 1996) and the use of the drug jasplakinolide also established that controlled actin polymerization contributes critically to the speed and directionality of motility (Wetzel *et al*., 2003). Recently, the demonstration of a connection between the microneme adhesive protein TgMIC2 and aldolase, an F-actin binding protein has provided a plausible first link between the microneme proteins and the parasite actin cytoskeleton. The inhibitor of myosin heavy chain ATPase 2,3-butanedione monoxime (BDM) was initially used to support the role of myosins for both gliding motility and invasion (Dobrowolski and Sibley, 1997) as was more recently confirmed by the conditional knockout of the small myosin motor TgMyoA (Meissner *et al*., 2002). TgMyoA motor complex is composed of the heavy chain, the light chain

* To whom correspondence should be addressed. Phone: +41-22-379-5672; Fax: +41-22-379-5702; E-mail: dominique.soldati-favre@medecine.unige.ch.

(TgMLC1) and two additional proteins TgGAP45 and TgGAP50 that serve as receptors and anchor the complex in the inner membrane complex (Gaskins *et al*., 2004). The determination of the topology of the motor in the parasite pellicle shed new light on the mechanism powering motility (Keeley and Soldati, 2004). *T. gondii* tachyzoites exhibit three complex types of myosin-dependent movements (Hakansson *et al*., 1999) and it is not known yet if TgMyoA is the only motor contributing to parasite motion.

Until recently, five unconventional class XIV myosins referred as MyoA to E were described in *T. gondii* (Heintzelman and Schwartzman, 1997; Hettmann *et al*., 2000). The complete sequencing and assembly of the *Toxoplasma* genome has recently revealed a repertoire of 11 myosins with one more motor named TgMyoH, which also belongs to the class XIV (Foth and Soldati, unpublished). The class XIV has been divided into three main subclasses (Lew *et al*., 2002). The subclass XIVa comprises the highly conserved apicomplexan homologues of TgMyoA in other apicomplexans and the very closely related myosin TgMyoD (Hettmann *et al*., 2000) that has most likely arisen from a gene duplication of TgMyoA and that has so far only been detected in the coccidian *T. gondii* and *Eimeria tenella*. Subclass XIVb consists of a more heterogeneous collection of related motors. This subclass includes TgMyoB and TgMyoC, which are the products of alternatively spliced transcripts from the same gene that differ only in their C-terminal tails. Overexpression of these myosins affects the integrity of the pellicle after parasite division (Delbac *et al*., 2001).

All class XIVa myosins are very short motor molecules that contain a divergent neck and lack a true tail domain. TgMyoA does not possess a recognizable IQ motif but the last 22 amino acids at the carboxy-terminus of the motor contribute to the association with the myosin light chain, TgMLC1 (Herm-Goetz *et al*., 2002). In *Plasmodium species*, the MyoA localizes also underneath the plasma membrane (Pinder *et al*., 1998; Margos *et al*., 2000; Matuschewski *et al*., 2001) and is associated at the C-terminus to a homologue of TgMLC1, MTIP (Bergman *et al*., 2003).

TgMyoD is the smallest *T. gondii* myosin identified so far, with a size of 91-kDa. Like TgMyoA it is distributed in the pellicle of tachyzoites and this localization is conferred by the extreme carboxy-terminus of the short carboxy-terminus, however TgMyoD shows a dottier but still peripheral staining. TgMyoD mutant lacking the tail domain is mainly cytoplasmic (Hettmann *et al*., 2000). The critical role of TgMyoA in gliding motility and host cell invasion was recently established through the generation of a conditional knockout for this gene with the assistance of an inducible expression system (Meissner *et al*., 2002). In this study, we have used the conventional homologous recombination strategy to produce a mutant lacking TgMyoD in the virulent strain RH. Our results on the phenotype of the mutant indicates that TgMyoD is not necessary for gliding motility and invasion and is not essential for survival of the tachyzoite stage. In addition, immunofluorescence labelling on the Prugniaud strain using anti-TgMyoD antibodies combined with RT-PCR analyses comparing tachyzoites and bradyzoites indicates that TgMyoD is not significantly present in tachyzoites but is produced in bradyzoites suggesting a specific role in the dormant stage. The transient kinetics data on TgMyoD confirm that this motor is similar to TgMyoA, namely a fast motor designed to generate movement rather than force.

Material and methods

Reagents

Restriction enzymes were purchased from New England Biolabs. The secondary antibodies for Western blotting were from Biorad, and for immunofluorescence from Molecular Probe.

Growth of parasites and isolation of DNA and total RNA

T. gondii tachyzoites (RH strain wild-type and RH*hxgprt*$^-$) were grown in human foreskin fibroblasts (HFF) maintained in Dulbecco's Modified Eagle's Medium (DMEM) supplemented with 10% fetal calf serum (FCS), 2 mM glutamine and 25 μg/ml gentamicine. Parasites were harvested after complete lysis of the host cells and purified by passage through 3.0 μm filters and centrifugation in PBS. Genomic DNA was isolated from purified parasites by sodium dodecyl sulfate/proteinase K lysis followed by phenol/chloroform, chloroform extractions and ethanol precipitation (Sibley *et al*., 1992).

Toxoplasma genomic library screening

A cosmid clone containing the myosin D locus was isolated from a cosmid library. The library was made in a SuperCos vector modified with SAG1/ble *Toxoplasma* selection cassette inserted into its *Hin*dIII site. The library was prepared from a *Sau*3AI partial digestion of RH genomic DNA ligated into the *Bam*HI cloning site and was kindly provided by D. Sibley and D. Howe. We partially sequenced the cosmid clone (H11–109) encompassing the TgMyoD locus (GenBank accession number AF105118).

Construction of T. gondii *vectors for* MyoD *gene replacement*

Plasmids for gene replacement were done as follows: the vectors pT5TgMyoD/cat and pT5TgMyoD/hxgprt were generated by cloning upstream and downstream regions of the *MyoD* coding sequence in pT/230CAT and 2855 (HXGPRT) plasmids, respectively. 2500 bps

of the *MyoD* 5′UTR were amplified from the genomic cosmid clone H11–109 using primers 468 (5′-ggggtacc-ctgctcttgcatcagctctttcg-3′) and 469 (5′-ggggtaccggatccg-gtagtaaggaaaccgacgcc-3′) both containing a *Kpn*I restriction site. A segment of the *TgMyoD* 3′UTR (1700 bps) was also amplified with primers 470 (5′-cg-ggatccttaattaacgaaggcgaagacgcatg-3′) and 471 (5′-ccag-gcggccgcctaagcggcgattcacaaggtc-3′) containing the sites *Bam*HI and *Not*I, respectively. All PCR amplifications were performed with the proofreading Pwo DNA polymerase. 3′UTR was first introduced between *Bam*-HI and *Not*I of pT/230-TUB5/CAT or 2855 down-stream of the *CAT* or *HXGPRT* selection cassettes. 5′UTR was then introduced into the *Kpn*I site of both vectors upstream of the selection marker.

Parasite transfection (RHhxgprt$^-$) *and selection of stable transformants*

To favor double homologous recombination, the plasmids were linearized with *Pvu*I and *Not*I for pT5CAT-MyoDKO and by *Not*I and *Nsi*I for pT5MyoD/hxgprt. *T. gondii* tachyzoites (RH*hxgprt*$^-$) were then transfected by electroporation as previously described (Soldati and Boothroyd 1993) using three different amounts of plasmid DNA 20, 40 and 60 μg. The chloramphenicol acetyl transferase (CAT) or the hypoxanthine–xanthine–guanine–phosphoribosyltransferase (HXGPRT) was used as positive selectable marker gene in presence of 20 μM chloramphenicol or mycophenolic acid and xanthine, respectively, and as described (Donald *et al*., 1996). Parasites were cloned by limiting dilution in 96 well plates and analyzed for the expression of the transgenes by genomic PCR and subsequently confirmed by Southern blot hybridization.

Screening for MyoD *knockout clones by PCR and Southern blot hybridization*

Genomic DNA was extracted from tachyzoites using a DNA extraction kit (Boehringer). For PCR amplifications, primers were designed to distinguish the clones containing gene replacements from those containing TgMyoD. Primers 532 (5′-GGCGATCCGTGTCT-GAGTG-3′) and 533 (5′-TTGCTGCTTGCGGCTT-GAG-3′) amplify a 250 bps fragment corresponding to the 3′ end coding region of *TgMyoD*. Primers 104 (5′-CCGGGCTGCAGGAGAAAAAAATCACTGGA-3′) and 105 (5′-CCGGGCCGATCGTTACGCCCCCGC-CCTGCCAC-3′) amplify the *cat* selection cassette. PCR were done according to standard procedures.

For Southern blotting, 200 ng of total genomic DNA from wild-type RH or some recombinant parasite clones (*myodko*) were digested with 40 U of *Sac*I or *Hin*dIII for 4 h, separated on 0.8% agarose gel and transferred onto a positively charged nylon membrane. *TgMyoD* probe was digoxigenin-dUTP labeled by PCR using the DIG High Prime Labeling Kit (Boehringer), with the primers 187 (5′-GAGAAAGACGGT TGTCATCCT-3′) and 192 (5′-CTCGGCAAGACGA TGGTAT-3′) covering 200 bps of the *TgMyoD* 3′end coding region and 250 bps of its 3′UTR. After overnight hybridization at 66°C, anti-DIG antibody-alkaline phosphate conjugate (1:10,000) and its chemiluminescent substrate CSPD were used for signal detection using the DIG system, according to the recommendations of the manufacturer (Boehringer).

Generation of polyclonal antibodies specific for TgMyoD

To generate anti-TgMyoD antibodies, two peptides were synthesized and coupled to keyhole limpet hemocyanin (KLH) according to the protocol of the manufacturer (Pierce). The first synthetic peptide corresponded to a region in the N-terminus part of TgMyoD (LQQVEPTADSQELTVQAKEVC*, aa 66–85) and the second one was designed in the short basic tail (C*VLKRAKQLSTGRAVPATRI, aa 788–806). The C* was inserted for coupling with KLH. Two rabbits were then immunized with 100 μg of each KLH-peptide in Freund's complete adjuvant for the first injection followed by 2 weeks intervals with again 100 μg per peptide mixed with incomplete adjuvant (Gebru) according to the KLH immunization instruction.

Immunoaffinity purification of the TgMyoD sera

Two milliliter of the sera raised against the N-terminal synthetic peptide (LQQVEPTADSQELTVQAKEVC) were immunoaffinity purified against 8 mg of the same peptide coupled to Affi-Gel 15 according to the protocol of the manufacturer (Bio-Rad). The sera raised against the TgMyoD tail peptide (CVLKRAKQLST-GRAVPATRI) were also affinity purified by using a preparative western blot technique against the TgMyoD recombinant tail expressed in *E. coli*. TgMyoDtail coding region (corresponding to the aa 641 to 822) was amplified by using the oligonucleotides 202 (5′-CGGGATCCGCAAACCTTGATGCCC GCTT-3′) and 216 (5′-GCGGATCCGATCAACATG CCTTTTGCC-3′), which introduce flanking *Bam*HI sites. The PCR product was *Bam*HI cloned into the pET3a vector (Novagen). The recombinant protein was expressed and purified under denaturating conditions with Ni–NTA resin according to the manufacturers protocol (Qiagen). 400 μg of the purified protein were loaded on a preparative 12% SDS-PAGE and electro-transferred onto a nitrocellulose membrane.

Western blot analysis of parasite lysates

SDS-polyacrylamide gel electrophoresis (SDS-PAGE) was performed using standard methods (Laemmli, 1970). Crude extracts from *T. gondii* tachyzoites were separated by SDS-PAGE. Western blot analysis was carried out essentially as described previously (Soldati

et al., 1998) using between 8 and 10% polyacrylamide gels run under reducing conditions with 100 mM DTT in the loading buffer. After electrophoresis, proteins were transferred to Hybond ECL nitrocellulose. For detection, the membranes were incubated with antibodies diluted in PBS, 0.5% Tween-20 and then with the affinity-purified horseradish peroxidase-conjugated goat anti-mouse IgG or goat anti-rabbit IgG (1:2000) and bound antibodies visualized using the ECL system (Amersham Corp.). Direct recording of chemoluminescent signals and densitometry by the Luminescent Image Analyser LAS-1000 (FujiFilm) allowed for quantification of signal intensities within a broad linear range.

Indirect immunofluorescence assay (IFA) microscopy

Intracellular parasites were grown in HFF on glass slides. The rapid freezing in ultra cold methanol with combined fixation and permeabilization was performed as described previously (Neuhaus *et al*., 1998). Slides were blocked for 20 min in PBS – 0.2% TritonX-100 with 2% FCS followed by 60 min incubation with the affinity purified anti-MyoD rabbit Sera (1:500). After extended washing the second step Antibodies were added goat anti-rabbit IgG (Alexa 488) (Molecular Probes) and incubated for 1 h at room temperature and washed. Slides were mounted in Vectashield and kept at 4°C in the dark. Confocal images were collected with a Leica laser scanning confocal microscope (TCS-NT DM/IRB) using a 100× Plan-Apo objective with NA 1.30. Single optical sections were recorded with an optimal pinhole of 1.0 micrometer (according to Leica instructions) and 16 times averaging. All other micrographs were obtained on a Zeiss Axiophot with a camera (Photometrics Type CH-250). Adobe Photoshop (Adobe Systems, Mountain View, CA) was used for image processing.

Purification of TgMyoDΔtail

His_8TgMyoDΔtail was purified as described previously for His_8TgMyoAΔtail (Herm-Goetz *et al*., 2002). However, 10 times more parasites were needed to purify a comparable amount of MyoD compared to MyoA.

Gliding motility assay

Freshly lysed parasites were harvested and resuspended in Hank's balanced salt solution without Mg^{2+}/Ca^{2+} (HBSS, Gibco) with 10 mM Hepes and 1 mM EGTA to a concentration of 1×10^6 parasites per ml. 12 mm round cover slips were coated overnight at 4°C with 50% FCS/PBS. Before use, they were washed once with PBS and overlaid with 100 ml of parasites for 10 min and incubated in a pre-warmed wet chamber at 37°C. After incubation, the parasite suspension was removed and the cover slips were fixed with 2.5% paraformaldehyde for 20 min. The trails were stained using anti-SAG1 monoclonal antibodies DG52.

Intracellular replication assay

Equal numbers of RH*hxgprt*$^-$ and *myodko* parasites were plated onto confluent HFF monolayers on coverslips and allowed to invade for 1 h. Parasites were then incubated for an additional 24 h. The coverslips were fixed with 4% paraformaldehyde in PBS for 15 min and permeabilized with 0.2% Triton-X 100 in PBS for 30 min. Samples were blocked with PBS containing 2% BSA. Parasites were labeled with rabbit polyclonal anti-MLC1 followed by Alexa488-conjugated goat anti-rabbit IgG. Coverslips were mounted and examined by immunofluorescence microscopy. The number of parasites/vacuole was counted blindly (100 vacuoles). The parasites replication was compared in three independent experiments.

Experimental infections in mice

Purified tachyzoites from the parental RH delta HXGPRT and the knock out MyoD were inoculated into groups of five female 8–9-week-old BALB/c mice at 20×10^1 or 10^3 parasites per mouse and monitored until death for 10 days.

Transient kinetic analysis

The kinetic assays of TgMyoA/TgMyoAΔtail were described previously (Herm-Goetz *et al*., 2002). A similar approach was taken here for the TgMyoDΔtail except that the TgMyoDΔtail quenched (by ~8–10%) pyrene fluorescence when binding to pyrene labelled actin and this signal was used in the transient kinetic assays. All experiments were completed in 130 mM KCl, 5 mM $MgCl_2$ and 20 mM MOPS at pH 7.0 and 20°C. Stopped-Flow Experiments were performed with a Hi-Tech Scientific SF-61 DX2 stopped flow spectrometer. Signals from the fluorescence of mant-ATP or pyrene actin were measured using an excitation wavelength of 365 nm with emission collected through a KV389 filter. Data were analysed using software provided by Hi-Tech.

Steady state basal and actin activated ATPase rates were measured using absorbance changes at 340 nm with the pyruvate kinase/lactate dehydrogenase coupled assay system (Norby, 1971). Detailed assay conditions: 100 mM KCl, 20 mM MOPS (KOH, pH 7.0), 1 mM $MgCl_2$, 0.5 mM ATP, 1 mM PEP (phosphoenol pyruvic acid), 0.5 mM EGTA, 0.15 mM NADH, 20 U/ml PK (pyruvate kinase) and 40 U/ml LDH (lactate dehydrogenase). The myosin concentration was 0.33 μM in an assay volume of 500 μl. BDM concentrations were adjusted by adding BDM (dissolved in DMSO) from a 5 M stock solution. The absorbance at 340 nm was monitored with a Varian Cary 50 spectrophotometer to detect the conversion of NADH to

NAD^+ (molar equivalent to the hydrolysis of ATP), and the Mg^{2+}-ATPase activity was determined following the decrease of the absorbance of the assay solution at 340 nm. The assays were carried out at 20°C.

Results

Myosin D is present only in coccidian parasites

The *T. gondii* unconventional myosin D (TgMyoD) was previously identified through the screening of a cDNA library (Hettmann *et al*., 2000). Further characterization of the whole gene was realized by sequencing of a genomic cosmid clone. More than 12 kbps spanning the *TgMyoD* locus were sequenced. The *TgM-D* gene exists as a single copy within the haploid genome of *T. gondii* and is interrupted by 10 introns of various sizes, ranging from 176 to 895 bps. The ORF is 2469-bp length and encodes a protein of 822 amino acids with a size of 91 kDa. Some sequences upstream and downstream of the coding region were also determined and used to design a vector for gene replacement by double homologous recombination. Availability of several complete apicomplexan's genomes sequences allowed the determination of the complete repertoire of myosin in those organisms. Homologue of TgMyoD could only be found in the closely related coccidian *Eimeria tenella*. The amino acids sequence comparison revealed 58% identities and 73% similarities between the two motors (Figure 1a). Homologues of MyoD are likely to be found also in other coccidians such as *Neospora caninum* and *Sarcocystis neurona*, however the sequence information for these parasites is very limited and no corresponding sequences are available to date.

Disruption of T. gondii *myosin D*

To investigate the role of the *T. gondii* myosin D, we undertook the disruption of the *TgMyoD* gene in the RH strain by gene replacement via double homologous recombination using either a *cat* or *hxgprt* selection marker. The pT5TgMyoD/cat plasmid was constructed by cloning 5′ and 3′ flanking regions of *TgMyoD* upstream and downstream a *cat* expression cassette, respectively. Fragments of 2.5 kbps of the 5′UTR and 1.7 kbps of the 3′UTR were used to assist double homologous recombination, which is not a favored event in *T. gondii*. A schematic map of the endogenous *TgMyoD* genomic locus and *cat* construct for gene knockout is shown in the Figure 1b. Successful disruption of *TgMyoD* was obtained in one clone using chloramphenicol selection. The lack of specificity of the anti-TgMyoD antibodies in indirect immunofluorescence assay hampered the use of this method to screen for knockout clones. A genomic PCR screen was used to discriminate between the clones in which integration of the plasmid occurred randomly or by homologous recombination at the *TgMyoD* locus. Evidence for targeting of the *CAT* cassette into the *TgMyoD* locus was demonstrated by PCR analysis using either primers specific of the *cat* gene and amplifying the 3′ end coding region of *TgMyoD* and only one out of 9 clones was negative for*TgMyoD* (data not shown). Subsequently, Southern blot hybridization was performed to confirm that the targeting construct had replaced the wild-type locus via a double crossing-over event. DNA from recombinant clones was digested with *Sac*I or *Hin*dIII and examined by Southern blot analysis using a digoxigenin-labeled probe encompassing the last 200 bps of the *TgMyoD* C-terminus coding region and 250 bps of its 3′UTR (Figure 1b). The DNA from the RH strain was digested and included as control in the same experiment. Consistent with homologous integration, the chromosomal *Sac*I fragment containing the *cat* gene is 4400 bps length. Furthermore, the 2634 bps size after *Hin*dIII digestion was as predicted for homologous integration. In comparison, *Hin*dIII and *Sac*I digestions yielded two fragments of 2154 and 3571 bps for RH wild type, respectively. When the integration of the vector was random in the genome (8/9 recombinant clones), which is the major recombination event in *T. gondii*, two bands were visible (3571 and 4400 bps for *Sac*I, and 2154 and 2634 bps for *Hin*dIII), one corresponding to the endogenous gene and the other to the non-homologous integration of one copy of the plasmid (data not shown). A similar construct (pT5TgMyoD/hxgprt) bearing 5′ and 3′ flanking regions of *TgMyoD* upstream and downstream of the *hxgprt* expression cassette was used to select for *myodko* mutants. Two out of 14 stable transformants analyzed had integrated at the*TgMyoD* locus through a replacement event (not shown).

TgMyoD is expressed in bradyzoites and only weakly in tachyzoites

The final confirmation of the replacement of *TgMyoD* by the *cat* gene was deduced from Western blot analysis. Because no specific antibodies were obtained when rabbits were immunized with a recombinant TgMyoD expressed in *E. coli*, anti-TgMyoD antibodies were produced against two different synthetic peptides of 20 amino acids, one corresponding to a specific region in the N-terminus part and the second specific of the short basic tail of TgMyoD. When protein lysates from wild-type parasites (RH and Prugniaud strains) were probed with anti-TgMyoD antibodies directed against the N-terminus peptide, a band of 91 kDa was detected (Figure 2a). This band is mainly present in proteins from the cyst-forming Prugniaud strain (lane 2). Only a faint signal is observed with RH wild-type (lane 4). As expected, TgMyoD is absent in protein extracts from the knockout clones (Figure 2, lane 5). The specificity of the anti-peptide antibodies was also assessed on proteins

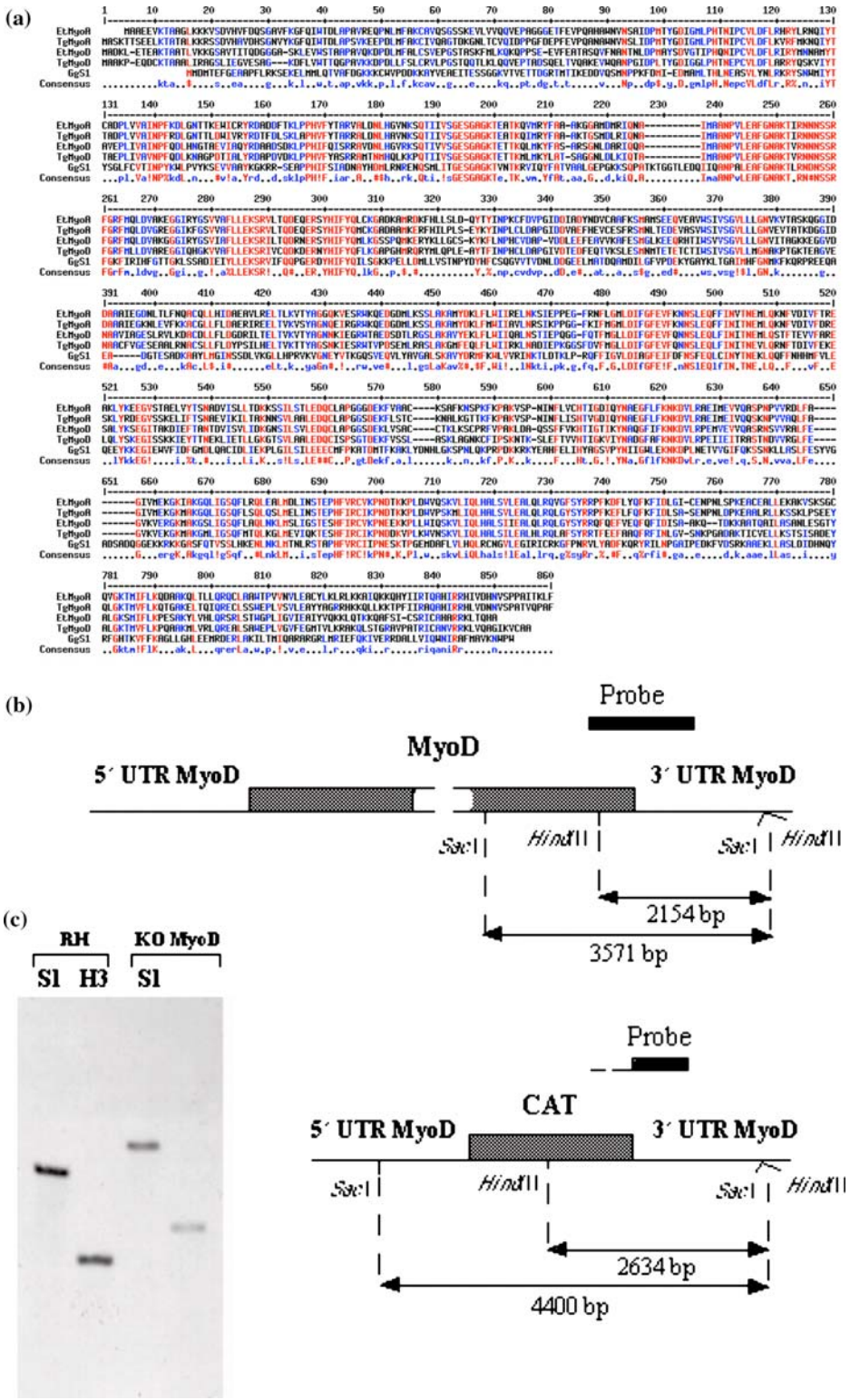

Fig. 1. (a) Amino acids sequence alignment of the TgMyoA (AF006626), TgMyoD (AF105118) EtMyoA Contig3535, EtMyoD Contig6876, myosin S-1 heavy chain, cardiac muscle - chicken (fragment JX0317). Red residues: 40% conserved or identical. Blue residues: 40% similar. TgmyoD/EtmyoD: Identities = 481/818 (58%), Positives = 599/818 (72%), Gaps = 8 /818 (0%). TgmyoA/EtMyoD: Identities = 482/822 (58%), Positives = 610/822 (73%), Gaps = 11/822 (1%). EtMyoA/EtMyoD: Identities = 475/814 (58%), Positives = 606/814 (74%), Gaps = 10/814 (1%). TgMyoA/EtMyoA. Identities = 612/825 (74%), Positives = 718/825 (86%). (b) Schematic genomic restriction map of the *TgMyoD* locus and of the *CAT* construct used for disruption of the *TgMyoD* gene. The plasmid pT5TgMyoD/cat used to disrupt TgMyoD contains 2.5 kbps of the 5′ and 1.7 kbps of the 3′ *TgMyoD* flanking sequences upstream and downstream of the *cat* selection marker. Only *Sac*I and *Hin*dIII restriction sites used to discriminate KO mutants from wild-type parasites are indicated. Thick black lines represent the digoxigenin labeled probe, spanning the 3′ end coding region of TgMyoD and 250 bps of its 3′ UTR. (c) Southern blot analysis of the wild type (RH) and the knockout clone (*myodko*). Genomic DNA was digested either with *Sac*I (S1) or *Hin*dIII (H3) and hybridized with the probe represented in Figure 1. In both case, only one fragment is detected in the wild type and the knockout clone reflecting the integration of cat by double homologous recombination.

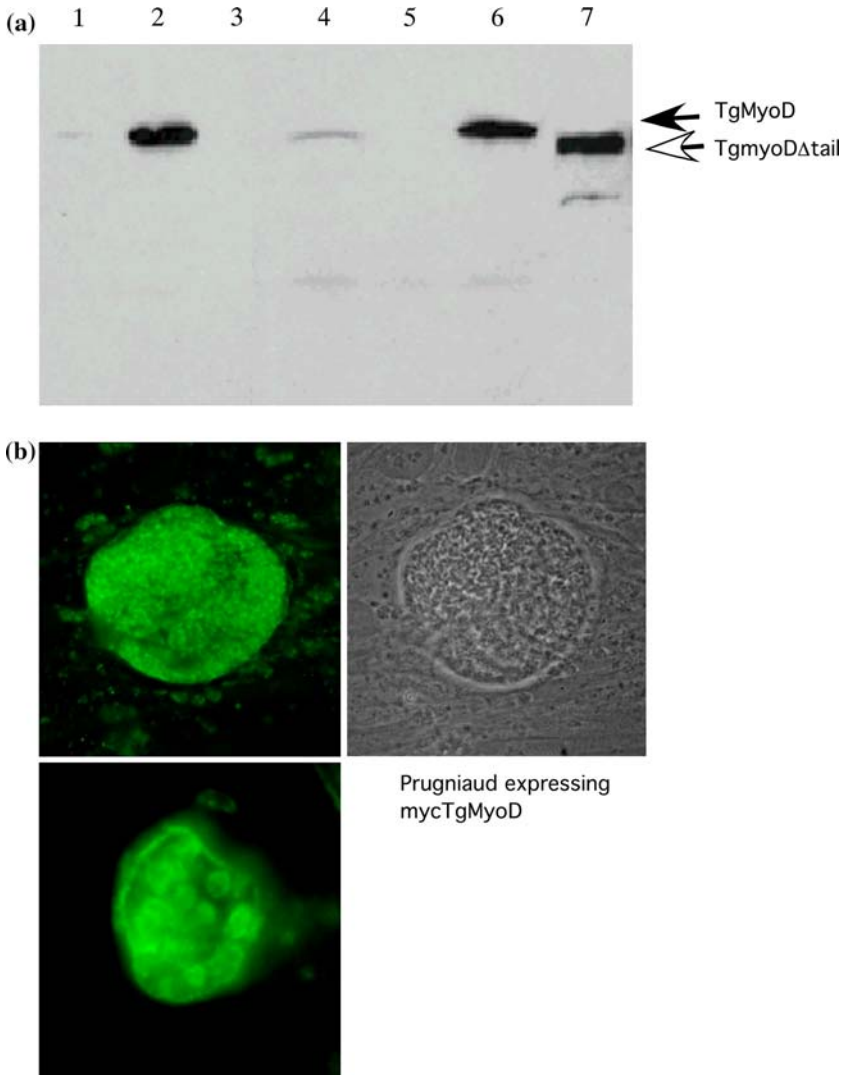

Fig. 2. (a) Western blot analysis. Prugniaud (lanes 1 and 2) and RH (lanes 3 and 4) wild-type strains, TgMyoD knockout (lane 5) and recombinant parasites expressing TgMyoD (lane 6) or TgMyoDΔtail (lane 7) were probed with antibodies directed against the N-terminus synthetic peptide from TgMyoD. The lanes were loaded with different amounts of freshly lysed parasites, from 10^6 (lanes 1 and 3 with RH) to 10^7 (lanes 2 and 4 with Prugniaud). TgMyoD was detected only when using 10^7 parasites, the signal being stronger with the Prugniaud strain (lane 2). As expected, no protein is detected from *myodko* mutant (lane 5). (b) IFA on Prugniaud strain in HFF cells.

from parasites stably expressing myc-TgMyoD or myc-TgMyoDΔtail, a construct lacking the last 57 aa corresponding to TgMyoDΔtail (Hettmann *et al.*, 2000). The signal observed on western blots from Prugniaud parasites suggests that TgMyoD is mainly expressed in the bradyzoites, the persistent and cyst forming stage of the parasite life cycle. This result confirms previous data reporting the level of mRNAs of the five known *T. gondii* myosins determined by semi-quantitative RT-PCR analysis. TgMyoA was constitutively expressed in tachyzoites and bradyzoites, whereas TgMyoD transcripts accumulated predominantly in bradyzoites (Delbac *et al.*, 2001). Initial efforts to obtain recombinant parasites expressing stable mycTgMyoD were unsuccessful, potentially because overexpression of this motor was not well tolerated by the parasites. To circumvent this problem, a weaker promoter was used. Expression level of transgenic myc-TgMyoD was significantly reduced compared with myc-TgMyoA expression (Hettmann *et al.*, 2000). Altogether these results argue for a role of TgMyoD in the bradyzoite stage.

TgMyoD is localized underneath the plasma membrane in cyst-forming Prugniaud strain

Previous studies by IFA, using recombinant parasites expressing a second copy of epitope myc-tagged full TgMyoD indicated that the motor was predominantly localized at the parasite periphery, consistent with a potential role of this myosin in gliding motility and invasion. In addition, truncation of MyoD C-terminal domain abolished the peripheral localization whereas GFP was targeted to the plasma membrane when fused to the TgMyoDtail (Hettmann *et al.*, 2000). Like for TgMyoA, this clearly indicates that the short basic C-terminus of TgMyoD is crucial for localization. Polyclonal antibodies recognizing MyoD were used to

stain *in vitro* cysts formed by the Prugniaud strain. A faint signal was detected in bradyzoites containing cysts confirming a distribution underneath the plasma membrane (Figure 2b). Antibodies directed against SAG4, a bradyzoite specific major antigen, were used as marker for the bradyzoite stage (Ödberg-Ferragut *et al*., 1996) (data not shown).

In vitro *analysis of the TgMyoD disrupted clones*

The knockout parasites were morphologically indistinguishable from wild-type parasites *in vitro* cell cultures. To determine if the absence of TgMyoD had phenotypic consequences, first a growth rate assay was performed. HFF cells were inoculated with different amounts (10^3 to 5.10^4) of tachyzoites from wild-type RH strain and *myodko* mutants for 30 min and washed. The number of tachyzoites per vacuole was determined 24 and 36 h later. The number of *myodko* parasites per vacuoles was not reduced compared with the wild type strain (Figure 3a).

To determine whether TgMyoD may have a role in gliding motility, *in vitro* motility assays were performed. A general feature of gliding motility in apicomplexan parasites is the formation of trails by gliding tachyzoites, which deposit surface membrane proteins on the solid surface. These trails can be easily detected by staining for surface components such as the major surface antigen SAG1. Figure 3b shows gliding Toxoplasma tachyzoites from wild type and myodko clones stained with a monoclonal antibody to SAG1. Both wild type and TgMyoD disrupted parasites left behind similar trials. Additionally, the *myodko* parasites showed no defect in gliding as monitored by time-lapse video microscopy (data not shown). These results led to the conclusion that the disruption of the *TgMyoD* gene did not affect parasite motility.

Host cell invasion and attachment were measured by adding the same number of freshly lysed wild type or *myodko* mutant parasites to HFF monolayers. After 1-h incubation at 37°C infected HFF cells were fixed and intracellular parasites were labelled with anti-MLC1 after permeabilization with 0.2% TritonX-100. The average numbers of intracellular parasites per scan area were counted. No significant differences were monitored between wild type and *myodko* parasites (Figure 3c). Additionally, the parasites cultivated for 5 days on HFF monolayers form plaques of comparable sizes (data not shown).

The absence of TgMyoD does not affect the parasite virulence in vivo

Mice were intraperitoneally infected with 1000 parasites (data not shown) or 100 parasites from wild type and *myodko* mutant and virulence was determined by the time necessary to kill the mice (Figure 3d). No significant difference was measured between wild type and *myodko* mutant strain.

His-myc-TgMyoDΔtail purification and biochemical analysis

In order to study the biochemical and biophysical properties of TgMyoD, we purified the motor from recombinant parasites expressing TgMyoDΔtail. His-tagged TgMyoD full length was only weakly expressed in tachyzoites and insoluble. In contrast a truncated version of this myosin TgMyoDΔtail corresponding to a deletion of the last 57 aa was produced in larger amount and could be purified using Ni-NTA resin column under native condition.

Kinetic data of MyoDΔtail

The rate at which myosin can detach from actin after completion of the work-part of the crossbridge cycle is often assumed to reflect the maximum velocity at which a myosin can move an actin filament (or along an actin filament). For most myosins this is controlled by either the rate at which ATP binds and induces dissociation of actin or by the rate of release ADP, which must occur before ATP can bind (Siemankowski and White, 1984; Weiss *et al*., 2001). Thus analysis of the rate of ADP release from actinTgMyoDΔtail and the rate of ATP induceddissociation of actoTgMyoDΔtail are of interest to compare with the values we previously recorded for TgMyoAΔtail.

*ATP induced dissociation of actin.TgMyo*D*Δ*tail

Unlike TgMyoA or TgMyoAΔtail, TgMyoDΔtail causes a small quench of the fluorescence of pyrene labeled actin (8–10%) and this is a more convenient signal to monitor the interaction with actin than the light scattering signal used for TgMyoAΔtail. The addition of an excess of ATP to 40 nM of phalloidin stabilized, pyrene-labelled actin resulted in complete dissociation of the actin from the complex. The signal change was well described by a single exponential and the observed rate constant (k_{obs}) was linearly dependent upon the concentration of ATP used in the range 5–100 μM. A plot of the ATP concentration dependence of the k_{obs} value is shown in Figure 4a and the slope of this line define the apparent second order rate constant of ATP binding. This is normally attributed to the product of the fast equilibrium binding of ATP (controlled by the equilibrium constant, K_1, Scheme II) and the rate constant for the protein isomerization, which leads to actin dissociation, k_{+2}. As can be seen from Table 1 the value of K_1k_{+2} is 2–3 times faster than the values measured for TgMyoAΔtail.

ADP inhibition of the ATP induced dissociation of acto.TgMyoDΔtail

Actin-TgMyoAΔtail binds ADP in a rapid weak equilibrium with an affinity (K_{AD}) of 350 μM. Thus ADP

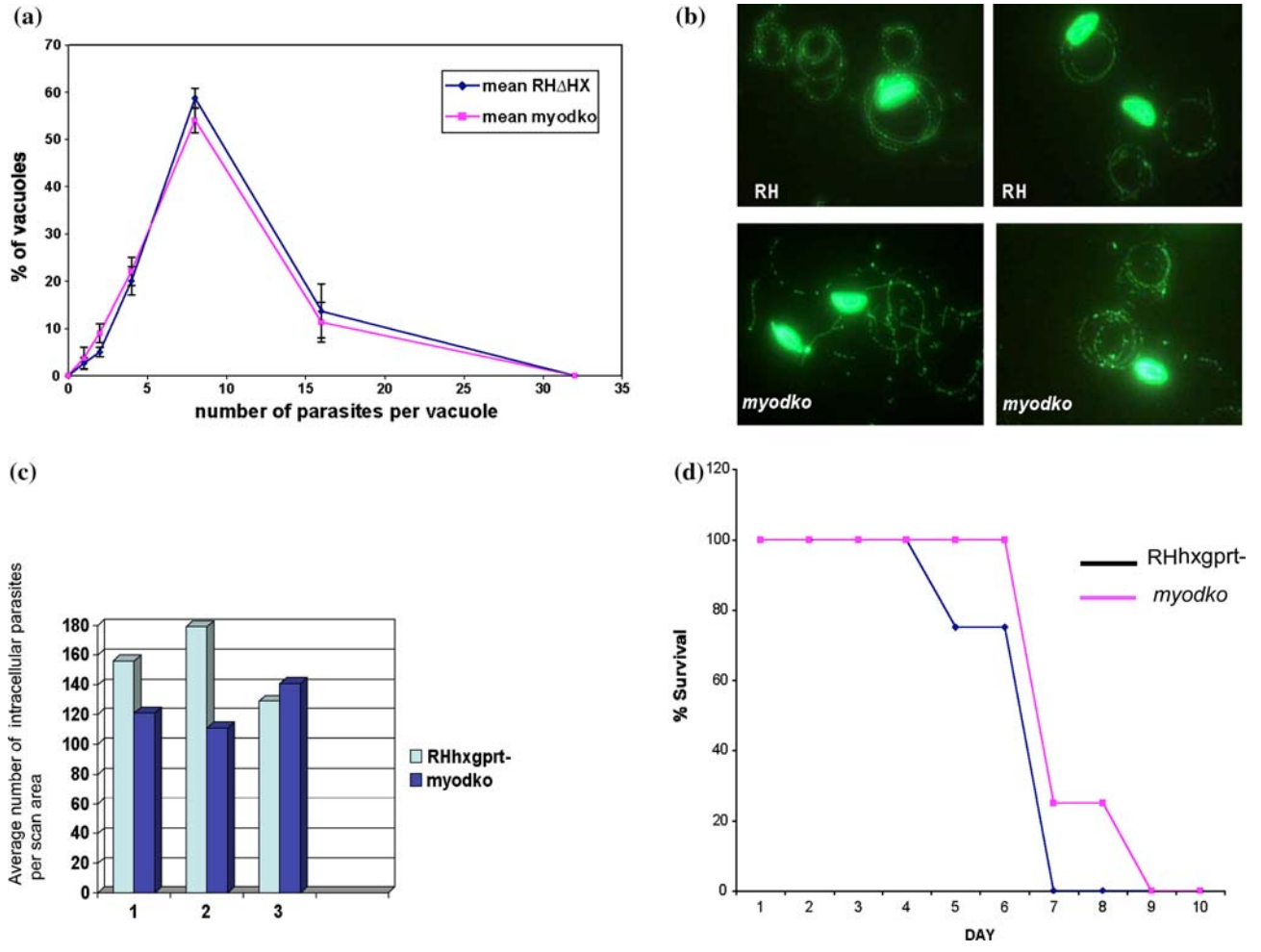

Fig. 3. (a) The absence of TgMyoD does not alter intracellular replication of the parasites. (b) *In vitro* gliding motility assay images of tachyzoites. Trails containing surface membrane proteins are visualized by staining with the monoclonal antibody DG52 directed against SAG1. No difference is observed between *myodko* and wild-type parasites. (c) TgMyoD does not play a significant role in host cell invasion by tachyzoites. (d) Purified tachyzoites from the parental*RHhxgprt*- and *myodko* inoculated into groups of five female 8–9-week-old BALB/c mice at 20×10^{1} parasites per mouse killed the animals with the same kinetics.

is a rapid competitive inhibitor of the ATP induced dissociation of actin from TgMyoAΔtail (Scheme II, Equation I). TgMyoDΔtail showed a similar behavior. When 40 nM actinTgMyoDΔtail was mixed with 50 μM ATP the observed rate of the dissociation reaction was slowed down by the presence of ADP. A plot of k_{obs} as a function of ADP concentration is shown in Figure 4b and indicated that k_{obs} is hyperbolically dependent upon ADP concentration. A fit of the data to Equation I gave a K_{AD} value of 105 μM. This is smaller than the value observed for TgMyoAΔtail but still indicates a rapid relatively weak equilibrium interaction between ADP and actin-TgMyoDΔtail. Although the figure shows the classic seven steps scheme for the interaction of myosin with nucleotides, only the nucleotide binding and release steps have been defined in the present study, and other steps are to be described in future investigations. Taken together the two measurements indicate that like TgMyoAΔtail, the TgMyoDΔtail is a classical muscle-type myosin with a relatively rapid interaction between nucleotide and actomyosin and suggests the myosins are both likely to be fast moving motors not designed for efficient force holding activity (see Nyitrai and Geeves, 2004).

*Mant.ATP binding to TgMyo*DΔtail

To complete this preliminary characterisation of the TgMyoDΔtail, we measured the rate of mant.ATP binding to TgMyoDΔtail in the absence of actin. For many myosins, this reaction can be followed using intrinsic protein fluorescence from the tryptophan residues in the sequence. However at the concentrations of TgMyoDΔtail available we could detect no measurable change in the intrinsic fluorescence on mixing with ATP. The W510 primarily responds to the open-to-closed transition associated with the switch-2 region and is often associated with ATP hydrolysis step rather than ATP binding (Geeves and Holmes, 1999; Malnasi-Csizmadia *et al.*, 2001). Both TgMyoA and TgMyoD lack this tryptophan (see Figure 1) and therefore there is no expectation of a fluorescence change on these steps. The fluorescence change associated with ATP

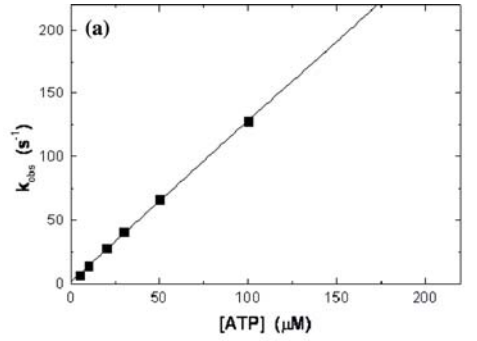

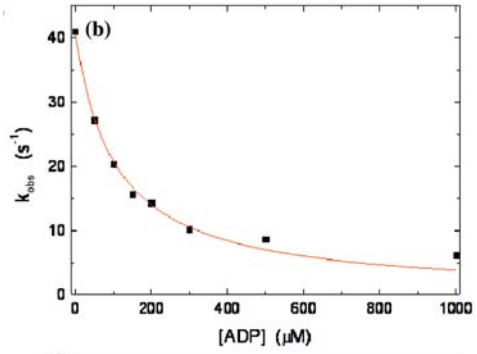

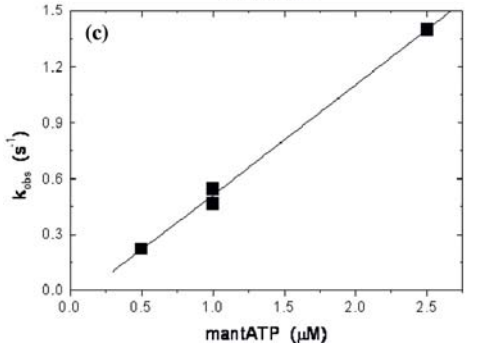

Scheme I

$$M + T \underset{k_{-1}}{\overset{k_{+1}}{\rightleftharpoons}} MT \underset{k_{-2}}{\overset{k_{+2}}{\rightleftharpoons}} M^*T \underset{k_{-3}}{\overset{k_{+3}}{\rightleftharpoons}} M^{**}DP \underset{k_{-4}}{\overset{k_{+4}}{\rightleftharpoons}} M^*DP \underset{k_{-5}}{\overset{k_{+5}}{\rightleftharpoons}} P + M^*.D \underset{k_{-6}}{\overset{k_{+6}}{\rightleftharpoons}} M.D \underset{k_{-7}}{\overset{k_{+7}}{\rightleftharpoons}} M + D$$

Scheme II

$$AM + T \underset{}{\overset{K_1}{\rightleftharpoons}} A.M.T \xrightarrow{k_{+2}} A\text{-}M.T \longrightarrow A + MT$$

$$+D \quad \underset{}{\overset{}{\rightleftharpoons}} \quad K_{AD}$$

$$A.M.D$$

Equation I: $$k_{obs} = \frac{k_{+2} \cdot K_1 \cdot [ATP]}{1 + [ADP]/K_{AD}}$$ ADP

Fig. 4 (a) Transient kinetic analysis of TgMyoDΔtail. The observed rate constant for the ATP induced dissociation of pyrene-actin.TgMyoDΔtail. ATP (at the concentrations indicated) was mixed in the stopped flow fluorimeter with 40 nM phalloidin stabilised pyrene-actin and 40 nM TgMyoDΔtail. The observed fluorescence transient was well described by a single exponential and the fitted k_{obs} values are plotted against the ATP concentration. The best fit line is superimposed and the slope defines the value of K_1k_{+2} (1.27 μM^{-1} s^{-1}) in Scheme II and Equation I. (b) The ADP inhibition of the ATP induced dissociation of pyrene-actin.TgMyoDΔtail. The reaction in B was repeated at a fixed ATP concentration of 50 μM with addition of ADP at the concentrations indicated to the ATP. The fluorescence transients were well described by a single exponential and the values of k_{obs} are plotted against the ADP concentration. The data are fitted to Equation I and gave a value of K_{AD} of 105 μM. (c) The binding of mantATP to TgM-DΔtail. Excess mantATP was mixed in the stopped flow fluorimeter with 150 nM TgMyoDΔtail and the mant fluorescence was observed. A single exponential described the observed transient and the graph plots k_{obs} against the mantATP concentration. A best-fit line to the data gives K_1k_{+2} (Scheme I) of 0.59 μM^{-1} s^{-1}. All measurements were performed at 100 mM KCl, 5 mM $MgCl_2$, 20 mM Mops at pH 7.0 and 20° C.

binding could originate with any one of the tryptophan residues in the structure.

On the other hand, the fluorescent ATP analogue mant.ATP gave reasonable signals as previously reported for TgMyoAΔtail. The signals could be observed either by exciting the mant directly at 365 nm or by exciting tryptophans and observing the fluorescence resonance energy transfer to the mantATP. Adding excess mantATP to 150 nM TgMyoDΔtail resulted in a fluorescence signal change that could be described by a single exponential and the k_{obs} values are plotted as a function of mant.ATP concentration in Figure 4c. This shows a linear relationship over the mant.ATP concentration range 0.5–2.5 μM the slope of the line is attributed to the apparent 2nd order rate constant of mantATP binding K_1k_{+2} in Scheme I. The value is very similar to that for TgMyoAΔtail.

To estimate the applicability of the coupled-enzyme assay for measuring the effect of BDM the Mg^{2+}-ATPase activity of rabbit skeletal S1 was measured in the absence of BDM, and in the presence of a series of BDM concentrations. The Mg^{2+}-ATPase activity observed in the absence of BDM (0.05 s^{-1}) decreased to ~40% at 70 mM BDM (Figure 5a). A hyperbolic fit to the Mg^{2+}-ATPase activity *vs.* BDM data gave a half saturation BDM concentration of 15.0 ± 1.6 mM. Organic solvents, such as DMSO, may have an effect on the biological activity of myosin. The Mg^{2+}-ATPase activity of skeletal S1 decreased to ~ 90% in the presence of 2% (v/v) DMSO, and to ~80% at 4%

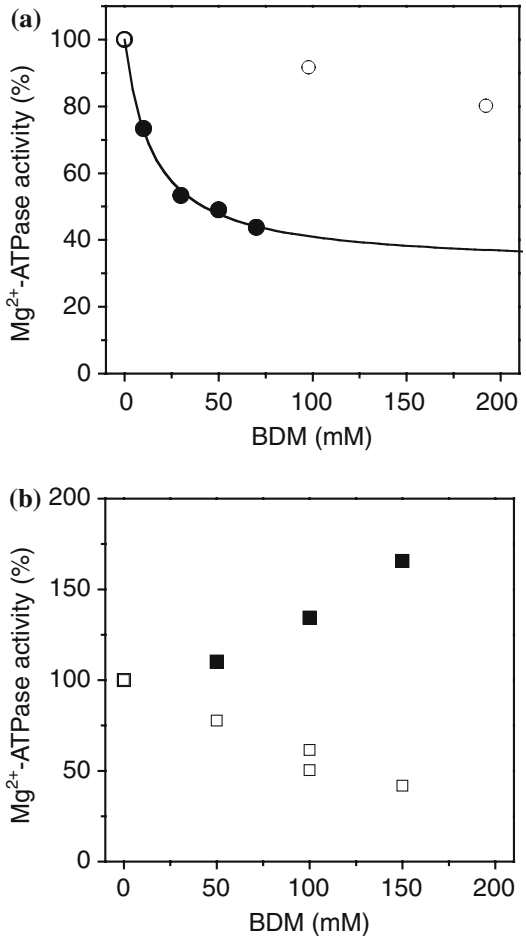

Fig. 5. The effect of BDM on the Mg^{2+}-ATPase of TgMyoAfull and TgMyoDΔtail. The figure shows the results of Mg^{2+}-ATPase experiments carried out using coupled-enzyme assay. (a) The Mg^{2+}-ATPase activity of rabbit skeletal S1 (0.47 μM) was measured as a function of BDM concentrations (filled circles). The data were normalised with the Mg^{2+}-ATPase activity of S1 measured in the absence of BDM (0.05 s^{-1}). Hyperbola fit to the data (solid line) gave half saturation BDM concentration of 15.0 ± 1.6 mM. BDM was dissolved in DMSO (5 M stock). The figure also shows the Mg^{2+}-ATPase activity of S1 in absence of BDM and in the presence of DMSO concentrations corresponding to the added DMSO amount at 100 mM and 200 mM BDM (empty circles). (b) The relative Mg^{2+}-ATPase activity of TgMyoAfull (0.4 μM) (filled squares) and TgMyoDΔtail (0.33 μM) (empty squares) as a function of BDM concentration. The data were normalised with the Mg^{2+}-ATPase activity measured in the absence of BDM (0.03 and 0.05 s^{-1} for TgMyoAfull and TgMyoDΔtail, respectively).

DMSO (Figure 5a). These DMSO concentrations correspond to the amount of the added solvent at 100 mM and 200 mM BDM, respectively. The results showed that the presence of DMSO could not account for the decrease of Mg^{2+}-ATPase activity of skeletal S1 observed after the additions of BDM. In the absence of BDM the Mg^{2+}-ATPase activity of TgMyoAfull and TgMyoDΔtail was 0.03 and 0.05 s^{-1}, respectively. These values are close to that observed with rabbit skeletal S1 (0.05 s^{-1}), and similar to the Mg^{2+}-ATPase activity of many other myosins. The Mg^{2+}-ATPase activity of TgMyoDΔtail decreased after the addition of millimolar concentrations of BDM (Figure 5b). The opposite BDM effect was observed in the case of TgMyoAfull (Figure 5b), where the Mg^{2+}-ATPase activity increased by ~63% at 150 mM BDM. The BDM dependence of the Mg^{2+}-ATPase activity appeared to be linear in the cases of both myosins.

Discussion

Apicomplexan parasites actively penetrate their host cell using an unusual form of substrate-dependent gliding motility, a process that requires the parasite actin cytoskeleton and at least one motor protein belonging to the myosin family. *T. gondii* actin was first shown to play a role in this process (Dobrowolski and Sibley, 1996) and a myosin is assumed to be required. Among the five *T. gondii* myosins so far identified, TgMyoB and TgMyoC have been shown to play a role in parasite division (Delbac *et al*., 2001). MyoA is the only motor strictly conserved throughout all the members of the phylum Apicomplexa. TgMyoA and the Plasmodium homologues were previously shown to localize beneath the plasma membrane of the tachyzoites and thus represented the primary candidate powering gliding locomotion and host cell penetration, a process essential for parasite survival. The development of an inducible system in *T. gondii* allowed the conditional disruption of the *TgMyoA* gene and proved to be essential for gliding (Meissner *et al*., 2002). However, it is still not clear how one motor protein powers three kinds of motions (Hakansson *et al*., 1999). The role of the closely related small myosin TgMyoD has not been assessed so far. In this report, we have examined the function and properties of TgMyoD in *T. gondii* tachyzoites and its potential role during host cell invasion. Although the haploid form of *T. gondii* facilitates the study of genes of interest by targeting gene disruption, it has been previously shown that vector integration in the genome occurs predominantly by non-homologous recombination. *T. gondii* mutants deficient in TgMyoD by gene disruption via double homologous recombination were obtained in 13% (1/9 and 2/14) of the recombinant clones.

Specific antibodies recognizing TgMyoD by Western blot analysis confirmed that the knockout clones failed to express TgMyoD and also established that TgMyoD is not significantly expressed in tachyzoites but instead in bradyzoites. Recombinant parasites expressing a tagged copy of TgMyoD indicated that the motor was distributed in punctuated pattern beneath the tachyzoite plasma membrane and the peripheral localization was confirmed in bradyzoites containing cysts *in vitro*.

In agreement with the faint expression or even absence of TgMyoD in tachyzoites, disruption of the gene revealed no characteristic phenotype in tachyzoites. Indeed, the *myodko* mutant showed no significant decrease in growth gliding and invasion. Unfortunately,

Table 1. Results of Transient Kinetic Analysis of TgMyoDΔtail

	Rate/equation constant	Units	TgMyoAΔtail	TgMyoDΔtail	Dicty MII ^{864}	$Ch^{sm}S1$	Rb^{st} S1
ADP binding to acto.M	K_{AD}	(μM)	350	105	94	5	200
ATP binding to acto.M	$K_1 \cdot k_{+2}$	(μM^{-1} s^{-1})	0.6	1.27	0.14	0.47	2.1
mantATP binding to M	$K_1 \cdot k_{+2}$	(μM^{-1} s^{-1})	0.65	0.59	0.70	nd	3.2
Basal ATPase	k_{cat}	(s^{-1})	0.063	0.05	0.08	nd	0.05

For comparison, TgMyoAΔtail (Herm-Goetz *et al.*, 2002), Dicty MII (Kurzawa *et al.*, 1997) $Ch^{sm}S1$ and $Rabbit^{st}$ S1 (Cremo and Geeves, 1998).

a possible role of TgMyoD in gliding in the bradyzoite stage cannot be investigated in the RH strain as this strain fails to differentiate *in vitro*. The *in vivo* experiments indicated that the parasites were as virulent as wild type and again the formation of cysts can not be assessed because this virulent strain induce a rapid death of the animals. Attempts to disrupt the corresponding gene in Prugniaud strain, which is more refractory to genetic manipulation, were until now unsuccessful.

Comparison of the kinetics of TgMyoD with TgMyoA and the muscle and cytoplasmic myosin II shown in Table 1 indicate that TgMyoD is a classic fast type myosin. ATP binds rapidly to actomyosin and dissociates actin from the complex and ADP is in a rapid reversible equilibrium with actomyosin. In contrast slow tension holding or tension sensing myosins such as members of myosin classes I, V, VI and slow members of the myosin II family have tightly bound ADP which can be only slowly released from actomyosin. See (Nyitrai and Geeves, 2004) for a more complete discussion.

2,3-Butanedione monoxime (BDM), is often cited in the parasitology field as a reversible myosin ATPase inhibitor and it was shown that BDM inhibits cell invasion by *T. gondii* and parasites gliding (Dobrowolski *et al.*, 1997). Such drugs gave hints that a myosin is involved in gliding and/or invasion. However, newer results studying different myosin classes (Acanthamoeba myosin-IC, human myosin I, chicken V and porcine myosin – VI) showed that BDM did not inhibit the Mg^{2+}-ATPase of non-rabbit skeletal myosin and therefore it should not be used in whole-cell experiments as a myosin inhibitor (Ostap, 2002). This and the fact that BDM is still often cited as a indicator for the involvement of a myosin in gliding and/or invasion prompted us to analyse the direct effect of BDM using two class XIV myosins, TgMyoAfull and TgMyoDΔtail. In the case of TgMyoA it was clearly shown that this myosin is a key player for invasion (Meissner *et al.*, 2002). Titration of BDM results in an apparently increase of the Mg-ATPase activity of TgMyoAfull. In contrast TgMyoDΔtail is slightly inhibited at higher concentrations. However, the ~50% inhibition at 100 mM BDM does not reflect an involvement of this myosin in gliding and/or invasion as TgMyoD KO showed no phenotype in tachyzoites. The facts that BDM in our *in vitro* experiments increased the Mg^{2+}-ATPase activity of TgMyoAfull, and only partially inhibited the Mg^{2+}-ATPase activity of TgMyoDΔtail even at relatively high (150 mM) concentration suggest, that the interpretation of the results from *in vivo* experiments where cells are treated with this drug is not straightforward.

In summary, we showed in this study that TgMyoD is not involved in gliding motility of tachyzoites as disruption of *TgMyoD* gene in RH strain revealed no phenotype compared to the wild type. This unconventional myosin seems to be mainly expressed in the dormant stage (bradyzoite form). It should be of interest to dissect the role of MyoD in other process through disruption of the gene in the Prugniaud strain. We have used recombinant tachyzoites expressing a His-tagged TgMyoD lacking the last 57 amino acids under the control of a constitutive promoter as a source for purification of this motor. We showed that this so far smallest analysed myosin is an active motor comparable with TgMyoA or other fast myosins. Like MyoA, this class XIV motor has some unusual structural features, but is a *bona fide* myosin. The kinetic and mechanical properties of TgMyoA are unexpectedly similar to those of fast skeletal muscle myosins. Combined microneedle–laser trap and sliding velocity assays established that TgMyoA moves in unitary steps of 5.3 nm with a velocity of 5.2 μm/s towards the plus end of actin filaments (Herm-Goetz *et al.*, 2002). TgMyoA monomer is associated with three other proteins, a myosin light chain TgMLC1 and the two gliding associated proteins TgGAP45 and TgGAP50 and is anchored to the inner membrane complex (Gaskins *et al.*, 2004). The dibasic motif in the last 22 amino acids is essential for the peripheral localization of TgMyoA is also conserved in TgMyoD. It is possible that TgMyoD uses the same light chain as TgMyoA, alternatively other MLC are present in the *T. gondii* genome and can represent the specific light chain for TgMyoD. It will be of interest to determine which proteins locate TgMyoD to the periphery of the parasites and unravel its role and importance in the persistent and problematic stage for the pathogenicity of Toxoplasmosis.

Acknowledgements

The sequence data (EtMyoD) were produced by BBSRC funded collaboration between the Pathogen Sequencing Unit at the Wellcome Trust Sanger

Institute and the Institute for Animal Health and can be obtained from http://www.genedb.org/genedb/etenella/. This work was mainly funded by the Deutsche Forschungsgemeinschaft. (DFG grant number SO 366/1–1, SO366/1–2) and the Wellcome Trust and Swiss National Fund to DS. AHG is currently supported by BioFuture (BMBF). Dr. F. Delbac was supported by a grant of the von Humboldt fundation. We thank Dr. Meissner for his cooperation.

References

Bergman LW, Kaiser K, Fujioka H, Coppens I, Daly TM, Fox S, Matuschewski K, Nussenzweig V and Kappe SH. (2003) Myosin A tail domain interacting protein (MTIP) localizes to the inner membrane complex of Plasmodium sporozoites. *J Cell Sci* **116:** 39–49.

Carruthers VB and Sibley LD (1997) Sequential protein secretion from three distinct organelles of *Toxoplasma gondii* accompanies invasion of human fibroblasts. *Eur J Cell Biol* **73:** 114–123.

Cremo CR and Geeves MA (1998) Interaction of actin and ADP with the head domain of smooth muscle myosin: implications for strain-dependent ADP release in smooth muscle. *Biochemistry* **37:** 1969–1978.

Delbac F, Sanger A, Neuhaus EM, Stratmann R, Ajioka JW, Toursel C, Herm-Gotz A, Tomavo S, Soldati T and Soldati D. (2001) *Toxoplasma gondii* myosins B/C: one gene, two tails, two localizations, and a role in parasite division. *J Cell Biol* **155:** 613–623.

Dobrowolski J and Sibley LD. (1997) The role of the cytoskeleton in host cell invasion by *Toxoplasma gondii*. *Behring Inst Mitt* **99:** 90–96.

Dobrowolski JM, Carruthers VB and Sibley LD. (1997) Participation of myosin in gliding motility and host cell invasion by *Toxoplasma gondii*. *Mol Microbiol* **26:** 163–173.

Dobrowolski JM and Sibley LD. (1996) Toxoplasma invasion of mammalian cells is powered by the actin cytoskeleton of the parasite. *Cell* **84:** 933–939.

Donald R, Carter D, Ullman B and Roos DS (1996) Insertional tagging, cloning, and expression of the *Toxoplasma gondii* hypoxanthine-xanthine-guanine phosphoribosyltransferase gene. Use as a selectable marker for stable transformation. *J Biol Chem* **271:** 14010–14019.

Gaskins E, Gilk S, DeVore N, Mann T, Ward G and Beckers C (2004) Identification of the membrane receptor of a class XIV myosin in *Toxoplasma gondii*. *J Cell Biol* **165:** 383–393.

Geeves MA and K.C. H. (1999) Structural mechanism of muscle contraction. *Ann. Rev. Biochem.* **68:** 687–728.

Hakansson S, Morisaki H, Heuser J and Sibley LD. (1999) Time-lapse video microscopy of gliding motility in *Toxoplasma gondii* reveals a novel, biphasic mechanism of cell locomotion. *Mol Biol Cell* **10:** 3539–3547.

Heintzelman MB and Schwartzman JD (1997) A novel class of unconventional myosins from *Toxoplasma gondii*. *J Mol Biol* **271:** 139–146.

Herm-Goetz A, Weiss S, Stratmann R, Fujita-Becker S, Ruff C, Meyhofer E, Soldati T, Manstein DJ, Geeves MA and Soldati D (2002) *Toxoplasma gondii* myosin A and its light chain: a fast, single-headed, plus-end-directed motor. *Embo J* **21:** 2149–2158.

Hettmann C, Herm A, Geiter A, Frank B, Schwarz E, Soldati T and Soldati D (2000) A dibasic motif in the tail of a class XIV apicomplexan myosin is an essential determinant of plasma membrane localization. *Mol Biol Cell* **11:** 1385–1400.

Keeley A and Soldati D (2004) The glideosome: a molecular machine powering motility and host-cell invasion by Apicomplexa Trends Cell. *Biology* **14:** 528–532.

Kurzawa SE, Manstein DJ and Geeves MA (1997) Dictyostelium discoideum myosin II: characterization of functional myosin motor fragments. *Biochemistry* **36:** 317–323.

Leammli UK (1970) Cleavage of structural protein during the assembly of the head of bacteriophageT4. *Nature* **227:** 680–685.

Lew AE, Dluzewski AR, Johnson AM and Pinder JC. (2002) Myosins of *Babesia bovis*: molecular characterisation, erythrocyte invasion, and phylogeny. *Cell Motil Cytoskeleton* **52:** 202–220.

Luft BJ and Remington JS (1992) Toxoplasmic encephalitis in AIDS. *Clin Infect Dis* **15:** 211–222.

Malnasi-Csizmadia A, Pearson DS, Kovacs M, Woolley RJ, Geeves MA and Bagshaw CR (2001) Kinetic resolution of a conformational transition and the ATP hydrolysis step using relaxation methods with a Dictyostelium myosin II mutant containing a single tryptophan residue. *Biochemistry* **40:** 12727–12737.

Margos G, Side'n-Kiamos I, Fowler RE, Gillman TR, Spaccapelo R, Lycett G, Vlachou D, G. P, Eling WM and, Mitchell GH, (2000) Myosin A expressions in sporogonic stages of Plasmodium. *Molecular and Biochemical Parasitology* **111:** 465–469.

Matuschewski K, Mota MM, Pinder JC, Nussenzweig V and Kappe SH (2001) Identification of the class XIV myosins Pb-MyoA and Py-MyoA and expression in Plasmodium. *Mol Biochem Parasitol* **15:** 157–161.

Meissner M, Schluter D and Soldati D (2002) Role of *Toxoplasma gondii* myosin A in powering parasite gliding and host cell invasion. *Science* **298:** 837–840.

Neuhaus EM, Horstmann H, Almers W, Maniak M and Soldati T (1998) Ethane-freezing/methanol-fixation of cell monolayers: a procedure for improved preservation of structure and antigenicity for light and electron microscopies. *J Struct Biol* **121:** 326–342.

Norby JG. (1971) Studies on a coupled enzyme assay for rate measurements of ATPase reactions. *Acta Chem Scand* **25:** 2717–2726.

Nyitrai M and Geeves MA (2004) Adenosine diphosphate and strain sensitivity in myosin motors. *Philos Trans R Soc Lond B Biol Sci* **359:** 1867–1877.

Ödberg-Ferragut C, Soete M, Engels A, Samyn B, Loyens A, Van Beeumen J, Camus D and Dubremetz J-F (1996) Molecular cloning of the *Toxoplasma gondii* sag4 gene encoding an 18 kDa bradyzoite specific surface protein. *Mol Biochem Parasitol* **82:** 237–244.

Ostap EM (2002) 2,3-Butanedione monoxime (BDM) as a myosin inhibitor. *J Muscle Res Cell Motil* **23:** 305–308.

Pinder JC, Fowler RE, Dluzewski AR, Bannister LH, Lavin FM, Mitchell GH, Wilson RJ and Gratzer WB (1998) Actomyosin motor in the merozoite of the malaria parasite, plasmodium falciparum: implications for red cell invasion. *J Cell Sci* **111:** 1831–1839.

Sibley LD, LeBlanc AJ, Pfefferkorn ER and Boothroyd JC (1992) Generation of a restriction fragment length polymorphism linkage map for *Toxoplasma gondii*. *Genetics* **132:** 1003–1015.

Siemankowski RF and White HD (1984) ADP dissociation from actomyosin subfragment 1 is sufficiently slow to limit the unloaded shortening velocity in vertebrate muscle. *J Biol Chem* **259:** 5045–5053.

Soldati D and Boothroyd JC (1993) Transient transfection and expression in the obligate intracellular parasite *Toxoplasma gondii*. *Science* **260:** 349–352.

Soldati D, Lassen A, Dubremetz JF and Boothroyd JC (1998) Processing of Toxoplasma ROP1 protein in nascent rhoptries. *Mol Biochem Parasitol* **96:** 37–48.

Weiss S, Rossi R, Pellegrino MA, Bottinelli R and Geeves MA (2001) Differing ADP release rates from myosin heavy chain isoforms define the shortening velocity of skeletal muscle fibers. *J Biol Chem* **276:** 45902–45908.

Wetzel DM, Hakansson S, Hu K, Roos D and Sibley LD (2003) Actin filament polymerization regulates gliding motility by apicomplexan parasites. *Mol Biol Cell* **14:** 396–406.